NMR time scale.[11] Thus, it is possible that the ammine adducts described here are also involved in exchange processes and that the observed NMR spectra represent time averages of spectra of several instantaneous structures. In an attempt to "freeze out" exchange processes, proton NMR spectra of **1** and **2** in chloroform-*d* solution were recorded at a series of temperatures from +50 to -60 °C. These present no definitive evidence for the occurrence of exchange but do not rule out the possibility that exchange is fast on the NMR time scale, even at -60 °C. Notable changes are observed only for two signals as the temperature is lowered. A broad signal at ~15 ppm, assigned[28] to 3-OH, sharpens for both **1** and **2**. Another signal at 6.4 ppm for **1** and 6.1 ppm for **2**, tentatively assigned to 22-OH by comparison with the spectrum of NaLAS,[11] shifts downfield by 0.3 ppm for **1** and decreases in intensity for **2** as the temperature is lowered. These changes are reversible for both adducts. If the assignment for 22-OH is correct, the changes observed are consistent with an ammine-LAS interaction at O_8, but further interpretation of the data would be unduly speculative.

In summary, LAS adducts of several Werner-type complexes are shown to have the stoichiometry [cation^{n+}](LAS)$_n$. The LAS anions are second-sphere ligands that are believed to interact with the cations via hydrogen bonds with ammine protons. The LAS anions remain bound to the cations in chloroform solution. The close similarity of carbon-13 NMR spectra of adducts **1** and **2** to that of the (*R*)-(+)-α-methylbenzylammonium cation indicates that O_3, O_6, and O_8 of LAS may be involved in hydrogen bonding. Carbon-13 spectra of the other adducts are sufficiently different from those of **1** and **2** to suggest a different pattern of hydrogen bonding. Low-temperature proton NMR experiments did not clearly reveal the occurrence of exchange processes involving the second-sphere ligands. It is possible that exchange among several instantaneous structures is fast on the NMR time scale. Instantaneous structures in which a given LAS anion is involved in hydrogen bonding to one or two transition-metal-coordinated ammine ligands seem plausible. These are illustrated schematically in Figure 2.

Registry No. **1**, 96243-09-3; **2**, 96243-10-6; **3**, 96243-11-7; **4**, 96243-12-8; **5**, 96243-13-9; **6**, 96243-14-0.

Contribution from the Division of Chemical and Physical Sciences, Deakin University, Waurn Ponds 3217, Victoria, Australia, and Department of Physical and Inorganic Chemistry, University of Adelaide, Adelaide 5001, South Australia, Australia

A Force Field for Molecular Mechanics Modeling of Cobalt(II) Amine Complexes and a New Model of Electron Transfer for Cobalt(III)-Cobalt(II) Redox Couples

A. M. BOND,*[1a] T. W. HAMBLEY,[1b,2] and M. R. SNOW*[1b]

Received October 16, 1984

A molecular mechanics force field for the description of cobalt(II)-hexaamine complexes is developed by modeling the cage complex $[Co^{II}(sepulchrate)]^{2+}$ and is applied to all isomers and conformers of the $[Co(dien)_2]^{3+/2+}$ system. The results for $[Co(dien)_2]^{3+/2+}$ correlate well with the observed reduction potentials of the different isomers. Relative energies of conformers are found to be quite different in the cobalt(III) and cobalt(II) states, and in some cases the global energy minima correspond to different conformational arrangements, which has implications for the electrochemical reduction of the cobalt(III) species. Conventionally, electrode processes involving reduction of cobalt(III) to cobalt(II) are treated as single step processes

$$Co(III) + e^- \overset{E^\circ, k_s, \alpha}{\rightleftharpoons} Co(II)$$

(E° = standard redox potential, k_s = heterogeneous rate constant for electron transfer, α = charge-transfer coefficient). However, when different conformational geometries are accessible and, especially, when the minima in free energy are associated with different conformers, the redox data cannot be treated via the use of the above equation. Rather a reaction of the kind (simplified)

$$\begin{array}{ccc} A_1 + e^- & \overset{E^\circ_1, (k_s)_1}{\rightleftharpoons} & A'_1 \\ \uparrow\downarrow K_1 & & \uparrow\downarrow K'_1 \\ A_2 + e^- & \overset{E^\circ_2, (k_s)_2}{\rightleftharpoons} & A'_2 \\ \vdots\ K_j & & \vdots\ K'_j \\ A_j + e^- & \overset{E^\circ_j, (k_s)_j}{\rightleftharpoons} & A'_j \end{array}$$

must be used, where A_j and A'_j represent conformers in different oxidation states and K_j and K'_j are equilibrium constants. It is concluded that many heterogeneous and homogeneous redox reactions will need to be reexamined to take account of conformational energy differences.

Introduction

Molecular mechanics modeling of metal complexes was first reported more than 15 years ago, and the majority of studies performed since then have concerned cobalt(III)-hexaamine complexes. We recently developed a revised force field, which has proved significantly more successful than previous models and facilitates extension of the method to metals other than cobalt(III).[3] A force field for cobalt(II) species is of particular interest; these complexes are generally kinetically labile and hence less accessible, yet their stabilities are important for understanding the Co(III)/Co(II) redox couples which have been the subject of extensive investigation.[4]

In almost all electrochemical investigations of cobalt(III)/cobalt(II) redox couples a simple model of electron transfer has been proposed (eq 1), in which the standard redox potential, E°, a

$$[Co(amine)]_x^{3+} + e^- \overset{E^\circ, k_s, \alpha}{\rightleftharpoons} [Co(amine)]_x^{2+} \qquad (1)$$

heterogeneous charge transfer rate constant, k_s, and a charge-

(1) (a) Deakin University. (b) University of Adelaide.
(2) Present address: School of Chemistry, University of Sydney, Sydney 2006, NSW, Australia.
(3) Hambley, T. W.; Hawkins, C. J.; Palmer, J. A.; Snow, M. R. *Aust. J. Chem.* **1981**, *34*, 45.
(4) Bard, A. J., Ed. "Encyclopedia of Electrochemistry of the Elements"; Marcel Dekker: New York, 1976.

0020-1669/85/1324-1920$01.50/0

transfer coefficient, α, are used to describe the reduction (oxidation) process. If the amine ligand is multidentate, it has been well established that the cobalt(III) complexes may exist in numerous conformers. For example the tris[(±)-1,2-propanediamine] cobalt(III) system has 24 isomers.[5] Equilibrium constants between different isomers/conformations have been calculated[5,6] and stabilities of the isomers have been rationalized with respect to the possible conformations that may be adopted by the 1,2-propanediamine rings.[5,6]

On the assumption of a single-step mechanism it has been argued by many workers[7] that structural change may be associated with slow electron transfer. Conversely, if no structure change accompanies electron transfer, then fast electron transfer (large k_s values) may be expected.

In a recent contribution[7] it was argued that if an alternative reaction scheme was operative in which structural change preceded or followed electron transfer and that a series of $E°$ values exist then a square reaction scheme (eq 2) is required to explain redox

$$\begin{array}{ccc} A_1 + ne^- & \overset{E^\circ_1,(k_s)_1}{\rightleftharpoons} & A'_1 \\ \uparrow\downarrow K_1 & & \uparrow\downarrow K'_1 \\ A_2 + ne^- & \overset{E^\circ_2,(k_s)_2}{\rightleftharpoons} & A'_2 \\ \uparrow\downarrow K_2 & & \uparrow\downarrow K'_2 \\ A_3 + ne^- & \overset{E^\circ_3,(k_s)_3}{\rightleftharpoons} & A'_3 \\ \uparrow\downarrow K_j & & \uparrow\downarrow K'_j \\ A_j + ne^- & \overset{E^\circ_j,(k_s)_j}{\rightleftharpoons} & A'_j \end{array} \qquad (2)$$

reactions involving structural change. Equation 2 represents a simplified version with α omitted for clarity and A_j and A'_j represent conformers in the different oxidation states. K_j and K'_j represent equilibrium constants between different conformers, although on the electrochemical time scale these reactions need not be in equilibrium. If this scheme is operative, theoretical studies clearly indicate that electrochemical (voltammetric) data should not be used to make deductions concerning structural changes accompanying charge transfer[7] as the mechanism is multistep rather than the one-step process implied by eq 1.

The fundamental difference between mechanisms described by reaction schemes 1 and 2 arises from the treatment of the standard redox potential, $E°$, term. In mechanism 1, a single $E°$ value must be used to describe a redox reaction, whereas in scheme 2 a continuum of $E°$ values may be required. The latter mode would seem to be essential when free energy differences exist between A_1 and A_j that are different from those between A'_1 and A'_j. In principle, it can be argued that the former scheme will only be appropriate when all conformers have equivalent free energy differences and that in reality this is simply a special subset of scheme 2. If this is not true, then any traditional treatment of electron transfer and structural change will be completely inadequate.

As part of our continuing work into providing appropriate models to redox processes involving (the possibility of) structural change, we have undertaken calculation of conformational energies of some cobalt amine complexes in both oxidation states III and II to determine the general suitability of reaction scheme 2. Cobalt amine redox couples have been examined in this context because the required X-ray crystallographic data are available. In particular, data on the kinetically stable cobalt cage complexes can be used as a model. Furthermore, substantial electrochemical data for the redox couple $[Co(dien)_2]^{2+}/[Co(dien)_2]^{3+}$ (dien = diethylenetriamine)[8] can be compared with predictions made from conformational energy calculations.

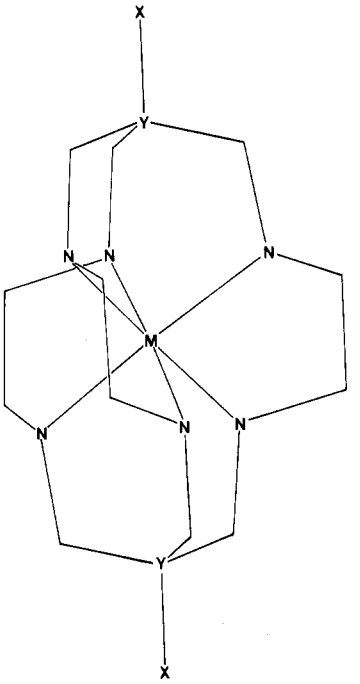

Figure 1. Schematic representation of [Co(hexaamine cryptate)].

Experimental Section

Cobalt(III) sepulchrate was prepared as the perchlorate salt with use of well-established literature methods.[9-11]

All polarographic data were recorded on Princeton Applied Research (PAR) Corp. Model 174 polarographic analyzers equipped with X-Y chart recorders. For dc and differential pulse measurements a mechanically controlled drop time of 0.5 s was used. The reference electrode was Ag/AgCl (saturated LiCl in acetone) separated from the test solution by a salt bridge containing the supporting electrolyte being used for the particular measurement, while the auxiliary electrode was a platinum wire. For cyclic voltammetry at a mercury drop electrode the scan was started 0.5 s after the commencement of drop formation.

Results and Discussion

The $[Co(sep)]^{3+}/[Co(sep)]^{2+}$ (sep = Sepulchrate) Redox Couple. (i) Molecular Mechanics. Sargeson and co-workers have prepared a series of hexaamine cryptate complexes of cobalt, rhodium, chromium, and platinum.[9-11] The so-called cryptate ligands encapsulate metal atoms as shown in Figure 1 and in so doing produce complexes with increased stability and inertness to substitution. Cobalt(III) sepulchrate complexes prepared by capping $[Co(en)_3]^{3+}$ molecules (en = ethane-1,2-diamine) are easily reduced to cobalt(II)[11,12] and remain nonlabile in contrast to Co(II) complexes of monodentate, bidentate, and even tridentate ligands. Thus the cage complexes of cobalt(II) sepulchrate can be crystallized and X-ray structural studies have been performed on both $[Co^{III}(sep)]^{3+}$[9] and $[Co^{II}(sep)]^{2+}$.[11] In each case, the complex has approximately D_3 symmetry with the three "ethylenediamine" rings adopting *lel* conformations. Consequently, this redox system can be used as a model for strain energy calculations since the cobalt(II) as well as cobalt(III) data are available. In the case of cobalt(II)[7] this is particularly important. For most other redox couples, data on the cobalt(II) oxidation state are unavailable because the complexes are too reactive. To generate a force field for cobalt(II) complexes, an energy minimization study of

(5) Harnung, S. E.; Kallesoe, S.; Sargeson, A. M.; Schäffer, C. E. *Acta Chem. Scand., Ser. A* **1974**, *A28*, 385.
(6) Dwyer, F. P.; Sargeson, A. M.; James, L. B. *J. Am. Chem. Soc.* **1964**, *86*, 590.
(7) Bond, A. M.; Oldham, K. B. *J. Phys. Chem.* **1983**, *87*, 2492 and references cited therein.
(8) Bond, A. M.; Keene, F. R.; Rumble, N. W.; Searle, G. H.; Snow, M. R. *Inorg. Chem.* **1978**, *17*, 2487.
(9) Creaser, I. I.; Harrowfield, J. M.; Herlt, A. J.; Sargeson, A. M.; Springborg, J.; Geue, R. J.; Snow, M. R. *J. Am. Chem. Soc.* **1977**, *99*, 3181.
(10) Sargeson, A. M. *Chem. Br.* **1979**, *15*, 23.
(11) Creaser, I. I.; Geue, R. J.; Harrowfield, J. M.; Herlt, A. J.; Sargeson, A. M.; Snow, M. R.; Springborg, J. *J. Am. Chem. Soc.* **1982**, *104*, 6016.
(12) Bond, A. M.; Lawrance, G. A.; Lay, P. A.; Sargeson, A. M. *Inorg. Chem.* **1983**, *22*, 2011 and references cited therein.

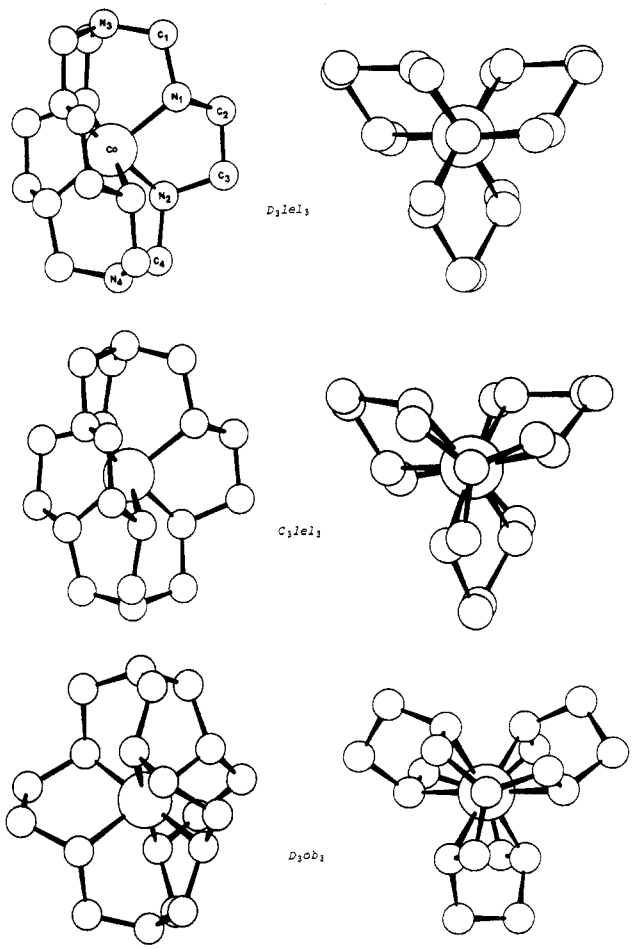

Figure 2. Energy-minimized conformers of $[Co(sep)]^{3+}$.

$[Co^{II}(sep)]^{2+}$ was undertaken and is described in detail. This model will subsequently be used for other cobalt(II) complexes in this and subsequent studies. An energy minimization study of $[Co^{III}(sep)]^{3+}$ will be described in detail elsewhere. Brief details are provided in this report.

The conformational isomerization of metal sepulchrate complexes arises from first the orientation of each capping moiety with respect to the rest of the ligand and second from the orientation of the three five-membered "en" rings. These latter rings can adopt conformations similar to those of $[Co(en)_3]^{3+}$ and hence are named, by analogy, *lel* and *ob* depending on whether the carbon–carbon vector of the ring is parallel to or at an angle to the cap to cap axis of the complex. In a previous molecular mechanics study of Co(III) sepulchrate three potential energy minima were located,[9] namely D_3lel_3, D_3ob_3, and C_3lel_3, where the first term refers to the overall symmetry of the complex and the second to the conformations of the "en" rings. Views of these energy-minimized Co^{III} geometries are shown in Figure 2. Conformers with both *lel* and *ob* ring orientations were not considered previously because it was considered that these would be less stable than the more symmetric geometries. However, in view of the statistical preference in solution for the lower symmetry conformers, we considered that these should also be subjected to molecular mechanics analysis.

The minimization methods and force field parameters employed in the present work were the same as those described previously.[3] Derivation of the additional force constants necessary for the modeling of cobalt(II) complexes and cage ligands is now described.

Our force field uses 1,3 nonbonded interactions to replace N–M–N angle deformation functions, and as a consequence, if we assume M–N–X angle functions are independent of metal ion, then the only metal-dependent function in the force field is that describing M–N bond length deformation. The force constant for the Co(II)–N bond deformation was taken from a normal-coordinate analysis of infrared spectroscopic data,[13] the same source as was used for the equivalent Co(III) function. The zero of the Co(II)–N bond was chosen to give the best fit for the $[Co^{II}(sep)]^{2+}$ complex and was checked by application to $[Co^{II}(NH_3)_6]^{2+}$, where the bond length was satisfactorily reproduced.

Table I. Additional Force Constants for Cobalt(II) Hexaamine Cryptate Complexes

bond length	k^r_{ij}, kJ mol^{-1} Å^{-1}	r^0_{ij}, Å
Co^{II}–N	494	2.120
C–C_{cap}	3012	1.540
C–N_{cap}	3012	1.440
valence angle	k^θ_{ijk}, kJ mol^{-1} rad^{-2}	θ^0_{ijk}, rad
Co^{II}–N–C	120	1.920
C–C–C_{cap}	271	1.911
C–C_{cap}–C	271	1.911
C_{cap}–C–H	217	1.909
N_{cap}–C–N	241	1.969
N_{cap}–C–H	146	1.911
torsion angle	v_{ij}, kJ mol^{-1}	**torsion angle** v_{ij}, kJ mol^{-1}
C–C_{cap}	1.15	C–N_{cap} 0.72

To fully model the $[Co(sep)]^{x+}$ complexes, functions were also required for the azo capping group. The N_{cap}–C bond length, averaged over three structure determinations, is 1.440 Å, and this value was used as r_0, with the force constant of a normal N–C bond chosen. The short nitrogen to carbon bond length suggests that a degree of sp^2 hybridization at the nitrogen is involved, and this raises the question as to what the zero of the C–N_{cap}–C valence angle is. A fully sp^2 hybridized nitrogen will be planar with a C–N–C angle of 120°, as observed in the solid-state structure of the macrobicyclic ligand $N[(CH_2)_2O(2,6\text{-}C_6H_3N)O(CH_2)_2]_3N$.[14] An sp^3 nitrogen will generally adopt a tetrahedral geometry (C–N–C = 109.4°) with a bond length of about 1.49 Å. However, the solid-state structure of the ligand diazabicyclopolyether (C-2.2.2.) exhibits short (mean 1.45 Å) carbon–nitrogen bond lengths but nonplanar geometry in the cap.[15] It seems probable that the NC_3 caps in these ligands are able to adopt whatever geometry best suits the constraints imposed by the remainder of the molecule, and it may be that the ratio of sp^2 to sp^3 hybridization varies to accommodate these changes. Thus in modeling these caps a force constant of zero for C–N_{cap}–C angle deformation was employed. This neutral force constant has successfully reproduced the C–N_{cap}–N angle in $[Co^{III}(sep)]^{3+}$, $[Co^{III}(azacapten)]^{3+}$, and $[Co^{II}(azacapten)]^{2+}$.[16] Torsional deformation terms involving the nitrogen atom of the bridgehead were calculated with the function used for terms involving saturated nitrogen atoms. A list of the force field parameters specific to the cobalt(II) cage complexes is given in Table I.

Starting coordinates were taken from the final $[Co(sep)]^{3+}$ coordinates. Refinement of these conformations, under the force field used here, proceeded easily to a true potential energy minimum in each case. C_3 symmetry only was imposed initially, with all symmetry constraints removed in the final stages of refinement, and it was found that in each case the final geometry strictly retained C_3 or D_3 symmetry. Starting coordinates for the mixed *lel*/*ob* geometries were derived by combining the final coordinates of the D_3ob_3 and both C_3lel_3 and D_3lel_3 conformers. In all cases refinement converged to one of the lel_2ob or ob_2lel conformers possessing C_2 symmetry, analogous to the lel_2ob and ob_2lel conformers of $[Co(en)_3]^{3+}$.

The Co(II) system of conformers gives strain energies (Table II) substantially different from those found for the Co(III) system, which are shown for comparison. The values for Co(II) are lower overall because of the larger Co–N bond and the reduced non-

(13) Nakagawa, I.; Shimanouchi, T. *Spectrochim. Acta* **1966**, *22*, 759.
(14) Newkome, G. R.; Majestic, V.; Fronczek, F. Atwood, J. L. *J. Am. Chem. Soc.* **1979**, *101*, 1047.
(15) Weiss, R.; Metz, B.; Moras, D. *Proc. Int. Conf. Coord. Chem., 8th* **1970**, *11*, 85.
(16) Hambley, T. W. Ph.D. Thesis, University of Adelaide, 1982.

Table II. Minimized Strain Energies of the $[Co(sep)]^{x+}$ Conformers (kJ mol^{-1})

conformer	E_b	E_{nb}	E_θ	E_ϕ	U_{total}	rel ΔH	rel ΔG
			$[Co^{III}(sep)]^{3+}$				
D_3lel_3	17.4	53.4	18.3	44.3	133.4	1.1	3.8
C_3lel_3	18.8	59.0	17.7	39.1	134.6	2.3	5.0
D_3ob_3	14.6	60.9	20.7	43.7	139.9	7.6	10.3
C_2lel_2ob	19.0	59.1	16.3	37.9	132.3	0	0
C_2ob_2lel	17.1	60.3	16.6	39.4	133.4	1.1	1.1
			$[Co^{II}(sep)]^{2+}$				
D_3lel_3	5.4	29.8	13.4	29.0	77.6	0	0
C_3lel_3	3.6	24.9	14.1	40.1	82.7	5.1	5.1
D_3ob_3	4.6	23.7	34.9	42.8	106.0	28.4	28.4
C_2lel_2ob	3.9	25.0	15.2	36.1	80.2	2.6	−0.1
C_2ob_2lel	4.1	24.3	23.0	39.0	90.4	12.8	10.1

Table III. Comparison of Observed and Calculated Structural Parameters for lel_3-$[Co(sep)]^{2+}$

	cryst structure[a]	energy minimized
Bond Lengths (Å)		
Co–N(1)	2.164 (12)	2.165
N(3)–C(1)	1.440 (14)	1.448
Valence Angles (deg)		
N(1)–Co–N(2)	81.9 (4)	79.7
N(1)–Co–N(1′)	89.1 (7)	87.1
N(1)–Co–N(2′)	101.7 (6)	111.2
Co–N(1)–C(1)	112.2 (8)	113.0
Co–N(1)–C(2)	106.6 (10)	109.6
N(1)–C(1)–N(3)	114.0 (11)	111.7
C(1)–N(1)–C(2)	113.4 (11)	113.2
N(1)–C(2)–C(3)	108.4 (11)	108.1
C(1)–N(3)–C(1′)	116.1 (13)	115.7
Torsion Angles (deg)		
Co–N(1)–C(1)–N(3)	12 (5)	25.3
Co–N(1)–C(2)–C(3)	−43 (3)	−41.8
N(1)–C(1)–N(3)–C(1′)	63 (4)	53.3
N(1)–C(1)–N(3)–C(1″)	−79 (3)	−86.6
N(3)–C(1)–N(1)–C(2)	130 (5)	150.6
C(1)–N(1)–C(2)–C(3)	−168 (3)	−169.0
N(1)–C(1)–C(2)–N(2)	60 (2)	55.4

[a] Observed values have been averaged by assuming D_3 symmetry.

bonded interactions in the consequently expanded ligand. The C_2lel_2ob and D_3lel_3 conformers are clearly the most stable while the D_3ob_3 conformer is again the least stable, to an even greater degree than for the Co(III) case. The major contributions to the total strain energy arise from different sources, and this also is due to the larger size of the Co(II) complex. The D_3lel_3 conformer has the largest contribution from nonbonded interactions but the least from torsional deformations. Expansion of this conformer on going from Co(III) to Co(II) has relieved the torsional distortions, and the torsion angle Co(1)–N(1)–C(1)–N(3) is 25.3° compared with 7.0° in the cobalt(III) case. A large valence angle deformation sum is observed for the D_3ob_3 conformer and is due almost entirely to distortions about the coordinated amine atoms. The C(1)–N(1)–C(2) angle is opened to 118.7°, corresponding to a strain energy of 3.5 kJ mol^{-1}, while Co–N(1)–C(1) is compressed to 102.2° (1.1 kJ mol^{-1}). These distortions are caused in part by the expansion of the molecule, and it is interesting to note that the D_3ob_3 conformer partially avoids this by being refined with a shorter Co–N bond (2.12 Å) than does the D_3lel_3 conformer (2.16 Å).

Table III gives a comparison between the energy minimized and crystal structure geometry details for the D_3lel_3 conformer of $[Co(sep)]^{2+}$. The solid-state geometry is again well reproduced, including that of the bridgehead group, suggesting that the Co(II) force field is valid. Thus, the force field, extended to enable modeling of $[Co^{II}(sep)]^{2+}$, is successful in terms of reproducing the details of the solid-state structure of the complex. Also the conformer found in that structure, D_3lel_3, has the lowest strain

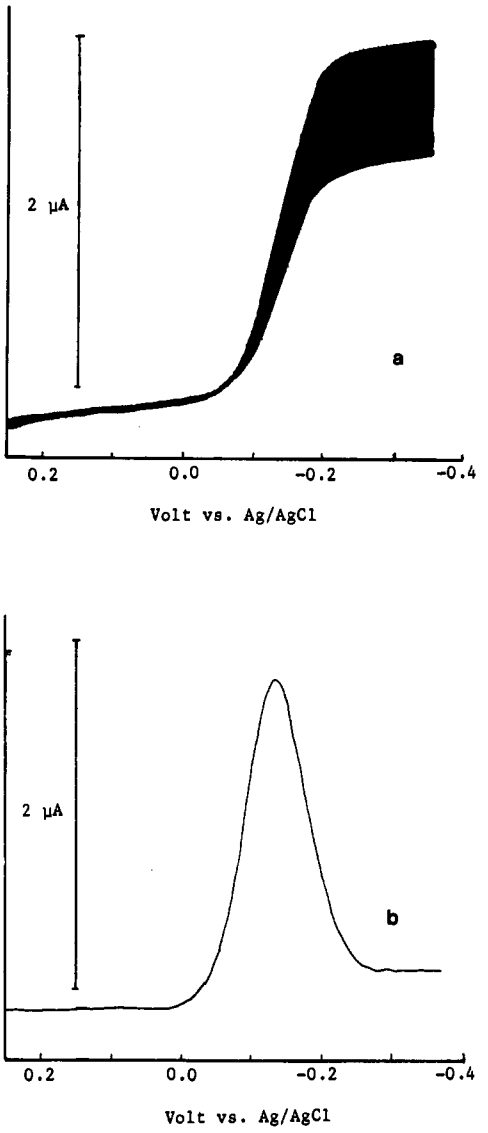

Figure 3. Dc (a) and differential pulse (b) polarograms of a 5×10^{-4} M solution of $[Co(sep)](ClO_4)_3$ in acetone (0.1 M Bu_4NPF_6). The pulse amplitude was −50 mV and drop time was 0.5 s.

energy, giving further confidence in the model for Co(II) systems.

(ii) Electrochemical Reduction of $[Co^{II}(sep)]^{3+}$. For this system only the D_3lel_3 conformer has been observed experimentally for cobalt(III). In view of the free energy data in Table II, if this conformational form is reduced to the cobalt(II) state, no energetically significant conformational changes are expected to occur on reduction and the electrochemical reduction from cobalt(III) to cobalt(II) can therefore be assumed to occur as in eq 3. If

$$D_3lel_3\text{-}[Co^{III}(sep)]^{3+} + e^- \overset{E^\circ_1,\, k_s}{\rightleftharpoons} D_3lel_3\text{-}[Co^{II}(sep)]^{2+} \quad (3)$$

the conformational change $D_3lel_3 \rightleftharpoons C_2lel_2ob$ occurs after electron transfer, the free energy change for the transformation would be so small that it could not be detectable electrochemically according to the calculations. Thus, this redox process is expected to be straightforward. Figure 3 shows a dc and differential pulse polarogram for reduction of $[Co^{III}(sep)_3]^{3+}$ in acetone (0.1 M Bu_4NPF_6), the same media for which data are available on the $[Co(dien)_3]^{3+/2+}$ system, and according to all accepted criteria of reversibility this is a diffusion-controlled reversible electron process at the dropping mercury electrode.[17,18] Thus $E_{1/2}$ is independent of drop time and a plot of log $(i_d - i)/i$ s. E (i =

(17) Bond, A. M.; Hanck, K. W. *J. Electroanal. Chem. Interfacial Electrochem.* **1981**, *129*, 89.
(18) Bond, A. M. "Modern Polarographic Methods in Analytical Chemistry"; Marcel Dekker: New York, 1980.

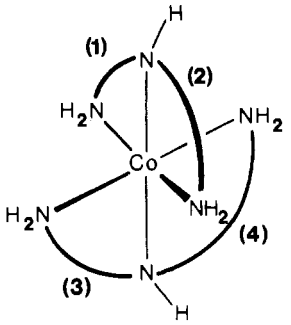

(a) δ-NH-*mer*

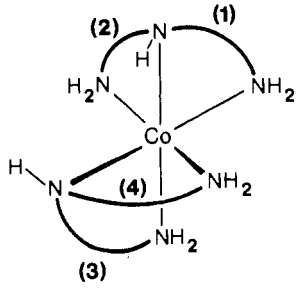

(b) Λ-*u*-*fac*

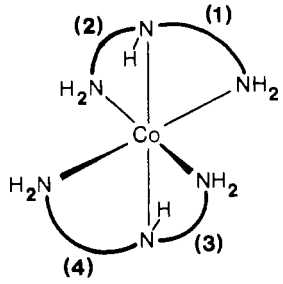

(c) *s*-*fac*

Figure 4. Schematic representations of the isomers of $[Co(dien)_2]^{3+}$ and ring numbering.

current, i_d = diffusion-controlled limiting current, E = potential) is linear with a slope of (57 ± 2) mV at 20 °C. The differential pulse peak potential is also more positive than $E_{1/2}$ by $-\Delta E/2$ mV as required (ΔE = pulse amplitude), and it has the shape expected[17] for the reversible one-electron process described by eq 3. Cyclic voltammograms also satisfy the usual criteria of reversibility.[18]

The $[Co(dien)_2]^{3+}/[Co(dien)_2]^{2+}$ Redox Couple. (i) Molecular Mechanics. The bis(tridentate) complex $[Co(dien)_2]^{3+}$ can exist in three geometric isomers: meridional (*mer*), unsymmetrical-facial (*u-fac*), and symmetrical-facial (*s-fac*), which are shown schematically in Figure 4. The three isomers were first isolated by Keene et al. in 1970.[19] The equilibrium isomer distribution has since been determined[20,21] as has the effect of environment on this distribution.[22] The results obtained in solutions with weakly associating anions all gave *mer*:*u-fac*:*s-fac* about 9:4:1.[20,22] Crystal structure analyses of all three isomers have been reported[23-25] with, in the case of the *u-fac* isomer, two conformations being observed in the solid state.[24]

Table IV. Minimized Strain Energies of the *mer*-$[Co(dien)_2]^{x+}$ Conformers (kJ mol^{-1})

conformer	sym	E_b	E_{nb}	E_θ	E_ϕ	U_{total}
(a) δ-*NH*-*mer*-$[Co^{III}(dien)_2]^{3+}$						
(δλ,δλ)	C_2	11.6	34.3	11.4	14.5	71.8
(λλ,λλ)	C_2	11.9	42.1	9.7	34.3	98.0
(λδ,λδ)	C_2	13.5	51.9	13.8	44.9	124.1
(λλ,δλ)	C_1	13.6	40.8	11.8	20.4	86.6
(λλ,λδ)	C_1	15.2	45.8	11.8	24.5	97.3
(b) δ-*NH*-*mer*-$[Co^{II}(dien)_2]^{2+}$						
(δλ,δλ)	C_2	2.7	16.8	7.9	10.1	37.5
(λλ,λλ)	C_2	4.1	24.9	8.4	14.8	52.2
(λλ,δλ)	C_1	3.4	21.6	8.1	12.6	45.7

Molecular mechanics studies of the three isomers of $[Co(dien)_2]^{3+}$ have previously been reported by two groups. Dwyer and Searle[26] employing the force field of Snow et al.[27,28] found that the *u-fac* and *s-fac* isomers had identical strain energies while that of the *mer* isomer was 1.7 kJ mol^{-1} higher. Yoshikawa,[29] using a similar force field, found that the strain energies of the *mer* and *s-fac* isomers differed by only 0.08 kJ mol^{-1} while the two conformers of the *u-fac* isomer they considered each had 0.25 kJ mol^{-1} more strain energy than the other isomers. These results are not in good agreement with the experimental isomer distributions, which suggest that the *mer* isomer is the most stable, by about 2 kJ mol^{-1} over the *u-fac* isomer and about 5 kJ mol^{-1} over the *s-fac* isomer. Also, these studies only considered the conformations that have been observed in the solid state. In view of the limited extent of these previous calculations, their apparent lack of success, and the significance of the system we have subjected all possible isomers and conformers of $[Co(dien)_2]^{3+}$ to analysis using the current force field. To generate data that is useful in studies of redox processes, the $[Co(dien)_2]^{2+}$ system was also examined.

***mer*-$[Co(dien)_2]^{3+}$ and *mer*-$[Co(dien)_2]^{2+}$.** A schematic representation of *mer*-$[Co(dien)_2]^{x+}$ with the ring-numbering scheme employed is shown in Figure 4a. Two optical isomers are possible, designated λ-NH or δ-NH according to the chirality of the *sec*-NH bonds in trans positions,[30] and the latter only is displayed in Figure 4a and considered hereafter. Each of the five-membered chelate rings can adopt δ or λ conformations,[30] giving four ligand conformations. These four, when applied to *mer*-$[Co(dien)_2]^{3+}$, generate 10 energetically distinct arrangements, which, for the δ-NH enantiomer, are as follows: (δλ,δλ), (λλ,λλ), (λδ,λδ), (δδ,δδ), (λλ,δλ), (λλ,λδ), (δδ,δλ), (δδ,λδ), (λδ,δλ), and (δδ,λλ), where the ring ordering follows that given in Figure 4a.

All 10 conformers were subjected to molecular mechanics analysis, the starting coordinates for (δλ,δλ) being derived from crystal structure coordinates[31] while the others were produced by using the program CART.[32] Potential energy minima were not obtained for many of the conformers, strain energy minimization leading to other conformers in these cases even when alternative sets of starting coordinates were tried. These failures were associated with strong interligand clashes or intraligand strain, and it is likely that potential energy minima do not exist for these

(19) Keene, F. R.; Searle, G. H.; Yoshikawa, Y.; Imai, A.; Yamasaki, K. *J. Chem. Soc. D* **1970**, 784.
(20) Keene, F. R.; Searle, G. H. *Inorg. Chem.* **1972**, *11*, 148.
(21) Yoshikawa, Y.; Yamasaki, K. *Bull. Chem. Soc. Jpn.* **1972**, *45*, 179.
(22) Keene, F. R.; Searle, G. H. *Inorg. Chem.* **1974**, *13*, 2173.
(23) Okiyama, K.; Sato, S.; Saito, Y. *Acta Crystallogr., Sect B: Struct. Crystallogr. Cryst. Chem.* **1979**, *B35*, 2389.
(24) Konno, M.; Marumo, F.; Saito, Y. *Acta Crystallogr., Sect. B: Struct. Crystallogr. Cryst. Chem.* **1973**, *B29*, 739.
(25) Kobayashi, M.; Marumo, F.; Saito, Y. *Acta Crystallogr., Sect. B: Struct. Crystallogr. Cryst. Chem.* **1972**, *B28*, 470.
(26) Dwyer, M.; Searle, G. H. *J. Chem. Soc., Chem. Commun.* **1972**, 726.
(27) Snow, M. R. *J. Am. Chem. Soc.* **1970**, *92*, 3610.
(28) Buckingham, D. A.; Maxwell, I. E.; Sargeson, A. M.; Snow, M. R. *J. Am. Chem. Soc.* **1970**, *92*, 3617.
(29) Yoshikawa, Y. *Bull. Chem. Soc. Jpn.* **1976**, *49*, 159.
(30) IUPAC. "Nomenclature of Inorganic Chemistry", 2nd ed.; Butterworths: London, 1971; pp 75–83.
(31) "ORTHOG, Programme for the Orthogonalization and Rotation of Crystal Coordinates": Maxwell, I., Australian National University, 1970.
(32) "CART, Calculation of Cartesian Coordinates from Internal Molecular Coordinates": Hilderbrant, R. L. *J. Chem. Phys.* **1969**, *51*, 1654.

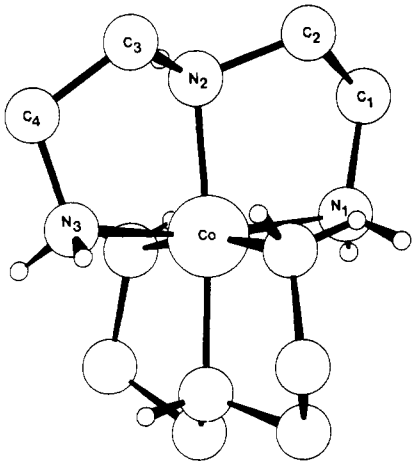

Figure 5. Energy-minimized (δλ,δλ)-*mer*-$[Co(dien)_2]^{3+}$.

geometries. The final strain energy totals for the successfully refined conformers are given in part a of Table IV for Co(III) and part b for Co(II). Fewer conformers were obtained for the Co(II) system as the larger N···N distance destabilizes the λδ ligand conformation by increasing intraring strain.

The (δλ,δλ) conformer has substantially lower strain energy than any other in both the Co(III) and Co(II) systems in accord with the observation of this geometry in the crystal structures of $(+)_{589}$-*mer*-$[Co(dien)_2]Br_3 \cdot 1.6H_2O$[23] and *mer*-$[Ni(dien)_2]Cl_2 \cdot H_2O$[33] (Ni(II) has M–N bond lengths similar to those of Co(II)). Also, the ^{13}C NMR spectrum of *mer*-$[Co(dien)_2]^{3+}$ indicates that in solution the meridionally coordinated dien lacks conformational freedom,[34] consistent with the energy minimization results, which show that only one conformation, (δλ,δλ), will be significantly populated in solution (Table IVa). The destabilization of conformers other than (δλ,δλ) rises primarily from torsional strain induced in the rings by unfavorable geometries. For example, the energy-minimized (λδ,λδ) geometry exhibits a near-eclipsed torsion angle Co–N(2)–C(2)–C(1) of 1.2°.

A PLUTO[35] plot of the energy-minimized (δλ,δλ)-*mer*-$[Co(dien)_2]^{3+}$ geometry is shown in Figure 5 with the atom-numbering scheme employed. Crystal structure analyses of two salts of *mer*-$[Co(dien)_2]^{3+}$ have been reported. However, the structure of the nitrate salt[36] has a number of inconsistencies, most notably a carbon–carbon separation of more than 2 Å in one ring while both atoms are at correct bonding distances from their associated nitrogen atoms. Therefore, for the purposes of comparison with the energy-minimized geometry, only results from the bromide structure[31] were used. Each asymmetric unit of the bromide salt contains three independent cations, and if we assume that C_2 symmetry that is strictly maintained in the energy-minimized structure, this gives six independent sets of geometrical parameters. These were averaged and were compared with those of the energy-minimized (δλ,δλ)-*mer* conformer in Table V. The large number of contributors to the solid-state geometry should serve to average out hydrogen-bonding effects, and generally excellent agreement with molecular mechanics results is observed.

***u-fac*-$[Co(dien)_2]^{3+}$ and *u-fac*-$[Co(dien)_2]^{2+}$.** A facially coordinated dien can only coordinate with one *sec*-N–H orientation; however, for the *u-fac* isomer two enantiomers are still possible (arising from the two relative orientations of the *sec*-NH groups) and the Λ enantiomer is represented schematically in Figure 4b. As with the *mer* isomer, each ligand can adopt 4 conformations, giving 10 energetically distinct arrangements when applied to the *u-fac* isomer.

Table V. Comparison of Observed and Calculated Structural Parameters for δ-*NH*-(δλ,δλ)-*mer*-$[Co(dien)_2]^{3+}$

	cryst structure[a]	energy minimized
Bond Lengths (Å)		
Co–N(1)	1.976 (13)	1.969
Co–N(2)	1.940 (16)	1.955
Co–N(3)	1.986 (9)	1.977
Valence Angles (deg)		
N(1)–Co–N(2)	84.9 (9)	84.9
N(2)–Co–N(3)	85.2 (7)	84.9
N(1)–Co–N(3)	169.9 (7)	169.4
Co–N(1)–C(1)	109.7 (15)	110.5
Co–N(2)–C(2)	109.2 (17)	108.0
Co–N(2)–C(3)	109.5 (8)	107.7
Co–N(3)–C(4)	109.1 (8)	110.2
N(1)–C(1)–C(2)	108.5 (4)	107.6
N(2)–C(2)–C(1)	104.8 (13)	105.2
N(2)–C(3)–C(4)	104.5 (11)	105.2
N(3)–C(4)–C(3)	108.9 (13)	107.8
C(2)–N(2)–C(3)	116.2 (7)	115.4
Torsion Angles (deg)		
Co–N(1)–C(1)–C(2)	−29 (4)	−29.9
Co–N(2)–C(2)–C(1)	−48 (3)	−48.2
Co–N(2)–C(3)–C(4)	46 (4)	49.1
Co–N(3)–C(4)–C(3)	32 (4)	29.3
N(1)–C(1)–C(2)–N(2)	49 (4)	50.2
N(2)–C(3)–C(4)–N(3)	−50 (3)	−50.4

[a] Observed values are taken from ref 23 and are averaged by assuming C_2 symmetry.

Table VI. Minimized Strain Energies of the *u-fac*-$[Co(dien)_2]^{x+}$ Conformers (kJ mol^{-1})

conformer	sym	E_b	E_{nb}	E_θ	E_ϕ	E_{total}
(a) Λ-*u-fac*-$[Co^{III}(dien)_2]^{3+}$						
(δδ,δδ)	C_2	12.4	39.7	7.3	22.2	81.6
(λλ,λλ)	C_2	12.5	39.1	8.1	21.6	81.3
(λδ,λδ)	C_2	10.6	35.3	8.4	24.8	79.1
(λλ,δδ)	C_1	13.3	40.3	8.0	24.1	85.7
(λδ,δδ)	C_1	11.7	38.1	8.0	23.3	81.1
(λλ,λδ)	C_1	12.1	38.8	8.5	23.4	82.8
(b) Λ-*u-fac*-$[Co^{II}(dien)_2]^{2+}$						
(δδ,δδ)	C_2	3.8	23.0	5.5	11.8	44.1
(λλ,λλ)	C_2	3.6	20.8	5.6	11.7	41.7
(λδ,λδ)	C_2	2.7	19.1	9.1	17.2	48.1
(λλ,δδ)	C_1	4.0	23.7	5.6	11.1	44.4
(λδ,δδ)	C_1	3.0	21.2	7.5	14.8	46.4
(λλ,λδ)	C_1	3.2	21.8	7.1	14.0	46.1

Again, all 10 conformers were subjected to energy minimization analysis, and in this case six were located as true potential energy minima for both the Co(III) and Co(II) systems. All conformers that failed to be refined had at least one δλ ligand conformation, and it is evident from Dreiding models that very strong intraligand nonbonded interactions destabilize this conformation. The δλ ligand conformation was obtained during energy minimization of the *s-fac* isomer (vide infra); however, when final coordinates taken from there were used as a starting point for the *u-fac* isomer, refinement again led to other conformations. Thus, interligand interactions must also play a role in the destabilization of the δλ conformation in the *u-fac* isomer.

Final strain energy totals for the refined *u-fac* conformers are given in part a of Table VI for Co(III) and part b for Co(II). The results for Co(III) show that no conformer is greatly preferred over the others, in contrast to the results obtained for the *mer* isomer. The arrangement of lowest strain energy (λδ,λδ) is one of those observed in the solid state while the other conformer found in that structure, (δδ,δδ),[24] has a strain energy 2.5 kJ mol^{-1} higher, a result not inconsistent with its occurrence. It is noteworthy that in the Co(II) case the most stable conformer is now (λλ,λλ) while the (λδ,λδ) arrangement is substantially destabilized, apparently by torsional strain induced by larger N···N distances.

(33) Biagini, S.; Cannas, M. *J. Chem. Soc. A* **1970**, 2398.
(34) Searle, G. H.; Lincoln, S. F.; Keene, F. R.; Teague, S. G.; Rowe, D. G. *Aust. J. Chem.* **1977**, *30*, 1221.
(35) "PLUTO, Programme for Crystal and Molecular Plotting": Motherwell, W. D. S., University of Cambridge, 1977.
(36) Sancilio, F. D.; Druding, L. F.; Lukaszewski, D. M. *Inorg. Chem.* **1976**, *15*, 1626.

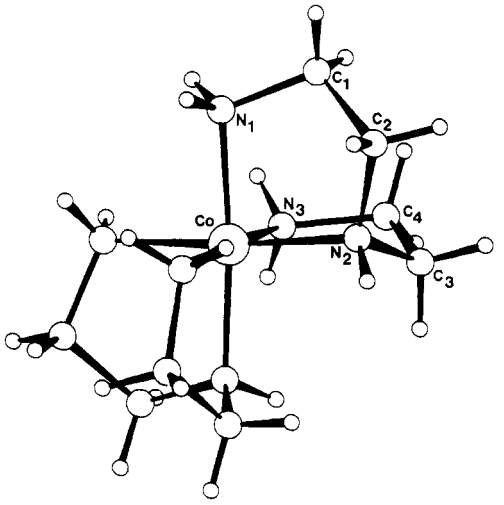

Figure 6. Energy-minimized (λδ,λδ)-*u-fac*-$[Co(dien)_2]^{3+}$.

Table VII. Comparison of Observed and Calculated Structural Parameters for *u-fac*-$[Co(dien)_2]^{3+}$

	Λ-(λδ,λδ)		(Λ-δδ,δδ)	
	cryst structure	energy minimized	cryst structure	energy minimized
	Bond Lengths (Å)			
Co-N(1)	1.957 (5)	1.960	1.951 (5)	1.963
Co-N(2)	1.970 (4)	1.962	1.968 (4)	1.975
Co-N(3)	1.969 (4)	1.968	1.970 (4)	1.974
	Valence Angles (deg)			
N(1)-Co-N(2)	86.4 (2)	87.4	85.7 (2)	85.0
N(2)-Co-N(3)	85.4 (1)	85.7	84.9 (1)	85.1
N(1)-Co-N(3)	91.3 (2)	92.2	92.8 (2)	94.9
Co-N(1)-C(1)	110.8 (3)	109.5	109.8 (4)	108.8
Co-N(2)-C(2)	109.3 (3)	108.6	110.3 (3)	111.5
Co-N(2)-C(3)	108.2 (2)	108.0	107.6 (2)	106.7
Co-N(3)-C(4)	111.8 (3)	112.1	111.8 (3)	111.4
N(1)-C(1)-C(2)	107.5 (5)	108.0	107.6 (4)	107.4
N(2)-C(2)-C(1)	110.2 (3)	110.3	109.9 (5)	109.3
N(2)-C(3)-C(4)	108.3 (4)	109.6	107.6 (4)	107.4
N(3)-C(4)-C(3)	108.0 (4)	108.1	106.4 (5)	106.9
C(2)-N(2)-C(3)	113.9 (5)	114.7	110.2 (5)	112.2
	Torsion Angles (deg)			
Co-N(1)-C(1)-C(2)	34.9	35.1	−41.1	−44.2
Co-N(2)-C(2)-C(1)	32.0	32.6	−24.9	−22.1
Co-N(2)-C(3)-C(4)	−43.1	−41.6	−45.4	−47.5
Co-N(3)-C(4)-C(3)	−26.0	−23.6	−18.2	−28.3
N(1)-C(1)-C(2)-N(2)	−43.4	−44.5	42.7	42.6
N(2)-C(3)-C(4)-N(3)	44.8	42.2	41.4	49.2

A PLUTO plot of the energy-minimized (λδ,λδ) geometry is shown in Figure 6. Both this conformer and (δδ,δδ) were observed in the solid-state structure of $(-)_{589}$-*u-fac*-$[Co^{III}(dien)_2][Co(CN)_6]\cdot 2H_2O$[24] with, in each case, the C_2 symmetry (strictly maintained in the energy-minimized geometries) crystallographically imposed. Comparisons between the details of these solid-state geometries and the relevant energy-minimized geometries are given in Table VII and show good agreement.

***s-fac*-$[Co(dien)_2]^{3+}$ and *s-fac*-$[Co(dien)_2]^{2+}$.** The *s-fac* isomer (Figure 4c) has potential point group symmetry C_{2h} and is not dissymmetric. A consequence of the higher symmetry (cf. *mer* and *u-fac*) is that the four possible ligand conformations when fitted to the *s-fac* isomer generate only seven energetically distinct arrangements (Table VIII). All seven were subjected to energy minimization analysis, and in the Co(III) case all were refined to true potential energy minima. For the Co(II) system only four conformers were refined, the λδ-*fac* ligand conformation again being unobtainable.

Of the Co(III) conformers, (λδ,λδ) has substantially lower strain energy (Table VIII) than any other, consistent with its occurrence in the crystal structure of *s-fac*-$[Co(dien)_2]Br_3$.[25] Large changes

Table VIII. Minimized Strain Energies of the *s-fac*-$[Co(dien)_2]^{x+}$ Conformers (kJ mol^{-1})

conformer	sym	E_b	E_{nb}	E_θ	E_ϕ	U_{total}
		(a) *s-fac*-$[Co(dien)_2]^{3+}$				
(λδ,λδ)	C_{2h}	9.9	35.2	8.7	25.9	79.7
(λλ,δδ)	C_i	13.7	47.8	8.4	28.4	98.3
(δλ,δλ)	C_{2h}	15.1	61.3	12.8	42.4	131.6
(λλ,λλ)	C_2	12.1	41.3	8.2	25.1	86.7
(δλ,λδ)	σ	14.3	53.7	10.0	37.0	115.0
(λδ,δδ)	C_1	11.9	40.8	7.9	26.1	86.7
(δλ,δδ)	C_1	14.7	54.6	10.0	35.0	114.3
		(b) *s-fac*-$[Co(dien)_2]^{2+}$				
(λδ,λδ)	C_{2h}	2.6	16.8	10.6	20.4	50.4
(λλ,δδ)	C_i	4.0	25.3	6.4	17.9	53.6
(λλ,λλ)	C_2	3.9	20.4	6.1	17.0	47.4
(λδ,δδ)	C_1	3.1	19.0	8.1	18.1	48.3

Table IX. Comparison of Observed and Calculated Structural Parameters for *s-fac*-$[Co(dien)_2]^{3+}$

	cryst structure[a]	energy minimized
	Bond Lengths (Å)	
Co-N(1)	1.97 (1)	1.966
Co-N(2)	1.95 (1)	1.950
	Valence Angles (deg)	
N(1)-Co-N(2)	86.9 (8)	87.6
N(1)-Co-N(3)	89.5 (5)	89.5
Co-N(1)-C(2)	110.7 (20)	110.3
Co-N(2)-C(2)	108.0 (12)	107.0
N(1)-C(1)-C(2)	108.6 (23)	108.6
N(2)-C(2)-C(1)	109.6 (16)	110.3
	Torsion Angles (deg)	
Co-N(1)-C(1)-C(2)	29 (2)	27.6
Co-N(2)-C(2)-C(1)	39 (2)	37.7
N(1)-C(1)-C(2)-N(2)	45 (2)	43.0

[a] Observed values are averaged by assuming C_{2h} symmetry.

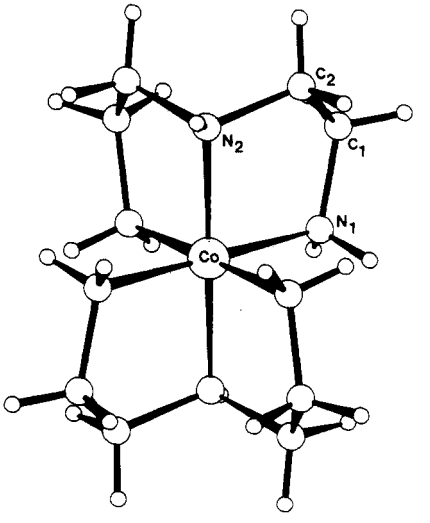

Figure 7. Energy-minimized (λδ,λδ)-*s-fac*-$[Co(dien)_2]^{3+}$.

in the relative strain energies are again observed on going from Co(III) to Co(II), and in the latter state the (λλ,λλ) conformer has the lowest strain energy though the lower symmetry (λδ,δδ) has a similar free energy in solution.

The low-energy (λδ,λδ) conformer was refined to a minimum energy geometry with strict C_{2h} symmetry (Figure 7). This is in contrast to previous energy minimization calculations on the (λδ,λδ)-*s-fac*-$[Co(dien)_2]^{3+}$ geometry,[37] where a maximum symmetry of C_i was obtained when it was refined free of constraints.

(37) Dwyer, M.; Geue, R. J.; Snow, M. R. *Inorg. Chem.* **1973**, *12*, 2057.

Table X. Calculated and Observed Free Energy Difference (kJ mol^{-1}) of the Isomers of $[Co(dien)_2]^{3+}$ and $[Co(dien)_2]^{2+}$

isomer and conformer	calcd rel ΔH	calcd rel ΔG	obsd rel ΔG acetone/ PF_6^- [a]	obsd rel ΔG DMA/ Me_2SO [b]	obsd rel ΔG H_2O/ Cl^- [b]
	(a) $[Co(dien)_2]^{3+}$				
δ-NH-(δλ,δλ)-*mer*	0	0	0	0	0
Λ-(λδ,λδ)-*u-fac*	7.3	7.3	3.6	4.2	2.0
(λδ,λδ)-*s-fac*	7.9	9.6	5.1	6.1	5.4
	(b) $[Co(dien)_2]^{2+}$				
δ-NH-(δλ,δλ)-*mer*	0	0	0		
Λ-(λλ,λλ)-*u-fac*	4.2	4.2	7.8		
(λλ,λλ)-*s-fac*	9.9	11.6	11.4		

[a] Data taken from ref 8. [b] Data taken from ref 22.

The solid-state structure of this geometry has C_i symmetry crystallographically imposed and approximates C_{2h} symmetry. A comparison of details of the crystal structure geometry, averaged by assuming C_{2h} symmetry, with those of the energy-minimized geometry is given in Table IX.

(ii) Electrochemical Reduction of $[Co(dien)_2]^{3+}$. The above conformational calculations enable predictions of redox processes to be made. For reduction of the *mer*-$[Co(dien)_2]^{3+}$ complex the process should essentially involve no conformational change and should be simple (eq 4). For the *u-fac* isomer all conformers

$$(\delta\lambda,\delta\lambda)\text{-}mer\text{-}[Co(dien)_2]^{3+} + e^- \underset{}{\overset{E^\circ_1,\,(k_s)_1}{\rightleftharpoons}} (\delta\lambda,\delta\lambda)\text{-}mer\text{-}[Co(dien)_2]^{2+} \quad (4)$$

exhibiting free energy minima have very similar strain energies in both cobalt(III) and cobalt(II) states. Consequently, the process will appear to be simple even if a conformational change did occur during charge transfer. That is, there may be a number of E°_j values but they will all be close to E°_2 used in eq 5. With the

$$u\text{-}fac\text{-}[Co(dien)_2]^{3+} + e^- \overset{E^\circ_2,\,(k_s)_2}{\rightleftharpoons} u\text{-}fac\text{-}[Co(dien)_2]^{2+} \quad (5)$$

s-fac isomer and for cobalt(III), the (λδ,λδ) conformer is obviously the most stable. On reduction to cobalt(II) the strain energies of all conformers are again very similar, and even if a conformational charge were to occur, the data would approximate that observed from a single E°_3 value. However, the most likely process is shown in eq 6.

$$(\lambda\delta,\lambda\delta)\text{-}s\text{-}fac\text{-}[Co(dien)_2]^{3+} + e^- \underset{}{\overset{E^\circ_3,\,(k_s)_3}{\rightleftharpoons}} (\lambda\delta,\lambda\delta)\text{-}s\text{-}fac\text{-}[Co(dien)_2]^{2+} \quad (6)$$

Thus, conformational changes, if indeed they occur, would not be expected to be measurable electrochemically. However, importantly, from the above calculations E°_1, E°_2, and E°_3 are predicted to be measurably different, as is known to be the case.

Keene and Searle have determined the equilibrium distribution of the three isomers of $[Co(dien)_2]^{3+}$ obtained under a range of environmental conditions.[22] In all cases where strongly or specifically associating anions were absent, the *mer* isomer was found to predominate over *u-fac* and *s-fac*. A typical result in water at 18 °C with chloride counter ion for the *mer*:*u-fac*:*s-fac* ratio was 65:28:7. The results obtained in aprotic solvents such as dimethyl sulfoxide or dimethylacetamide showed an even greater preference for the *mer* isomer. These isomer distributions can be used to calculate free energy differences between the isomers as shown in eq 7 with similar equations for other pairs of isomers.

$$\Delta G^\circ_{mer} - \Delta G^\circ_{u\text{-}fac} = -RT \ln ([mer]/[u\text{-}fac]) \quad (7)$$

The differences so calculated, with *mer*-Co(III) assigned as an arbitrary zero, are given in Table Xa. Strain energy differences correspond to enthalpy differences, and therefore before comparison with free energies can be made, corrections for statistical contributions to the entropy must be applied. Both the *mer* and *u-fac* isomers are dissymmetric, each able to adopt either of two enantiomeric geometries, and hence have a 2:1 preference over the centrosymmetric *s-fac* isomer. This corresponds to an energy difference of 1.7 kJ mol^{-1} (RT ln (2/1), T = 291 K), which must be added to the enthalpy of the *s-fac* isomer (Table Xa).

Satisfactory agreement between molecular-mechanics-produced free energies and those derived from the equilibration experiments is obtained (Table Xa). While the values are not exactly reproduced, the correct order of stabilities is, in contrast to previous energy minimization studies of the $[Co(dien)_2]^{3+}$ system,[26,29] where different force fields were used.

Bond et al. measured the potentials (E°_j) for Co(III) to Co(II) reduction for each of the three isomers of $[Co(dien)_2]^{3+}$ in acetone with 0.1 M Bu_4NPF_6 electrolyte.[8] They also determined the Co(III) isomer distribution in the same environment (Table Xa) and then calculated the isomer distribution in the Co(II) state using the relationship (8) and similar equations for other isomer

$$K_1 = \frac{[u\text{-}fac\text{-Co(III)}][mer\text{-Co(II)}]}{[mer\text{-Co(III)}][u\text{-}fac\text{-Co(II)}]} = \text{antilog}\,\frac{nF(\Delta E^\circ)}{2.303RT} \quad (8)$$

pairs. Applying eq 8 to the known Co(III) equilibrium distribution give the free energy differences for the Co(II) state. These are given in Table Xb with *mer*-Co(II) chosen as an arbitrary zero. The molecular-mechanics-calculated strain energy differences (again corrected for statistical effects) for the Co(II) system are also shown in Table Xb for comparison. The major change in isomer distribution on going from Co(III) to Co(II), as shown by the electrochemical measurements, is an increase in the degree of preference for the *mer* isomer. The strain energy differences reproduce this in the case of *mer*:*s-fac*, and overall reasonable agreement between the theoretical and experimental free energies is observed. The agreement between calculated and observed values emphasizes that the more complex model is essential and that a single one-step approach

$$\text{Co(III)} + e^- \overset{E^\circ,\,k_s}{\rightleftharpoons} \text{Co(II)}$$

is inadequate.

(iii) Effects of Ion Association. It is well established that ion association and solvation can affect isomer distributions. Keene and Searle[22] showed that the presence of an oxyanion such as phosphate or sulfate in an equilibration experiment greatly alters the distribution of the three isomers of $[Co(dien)_2]^{3+}$. For example, in water containing 0.08 M Na_3PO_4 the *mer*:*u-fac*:*s-fac* ratio observed was 20:25:55,[22] which represents a reversal in the preferences observed when only 0.02 M chloride was present. It could be argued therefore that the isomer preferences obtained from experimental data need not reflect calculated thermodynamic energy differences between the isomers which do not include terms for ion pairing. However, it should be noted that anions such as phosphate or sulfate apparently associate in a specific manner with the $[Co(dien)_2]^{3+}$ isomers and consequently stabilize one or the other of them. In fact a correlation between the ability of these anions to associate with a given isomer and the stabilization of that isomer can be demonstrated.

Searle[38] has shown that a correlation exists between ion association and elution rates on SP-Sephadex chromatography columns for the cations and anions described above. Thus elution rates (R_x) might be used as an approximate measure of ion association as long as complex–resin interactions remain of secondary importance.

The $[Co(dien)_2]^{3+}$ isomer distribution (*mer*:*u-fac*:*s-fac*) found in the presence of 0.08 M Na_3PO_4 (20:25:55)[22] when compared to the distribution observed in water with chloride counterion (65:28:7) shows an increased preference for *u-fac* over *mer* equivalent to 2.6 kJ mol^{-1} and for *s-fac* over *mer* equivalent to 7.8 kJ mol^{-1}. These results can be compared to the relative elution rates for the same isomers of 2.8 and 8.8. No significance can be attached to the near-coincidence of the numbers as different units and zeros apply; however, a close correlation between stabilization of an isomer by an anion and the isomer–anion association, as determined by relative elution rates, is clearly demonstrated. A similar correlation is observed for 0.2 M Na_2SO_4,

(38) Searle, G. H. *Aust. J. Chem.* **1977**, *30*, 2625.

where stabilization of *u-fac* and *s-fac* over *mer* correspond to 1.3 and 3.2 kJ mol^{-1}, respectively, compared to R_x values, derived from Figure 3 of ref 40, of 1.3 and 1.9.

These correlations suggest that if a given anion does not produce separation of the different isomers when used to elute a mixture down a column (i.e. $R_x \simeq 1$) then ion association with each isomer is similar and large environmentally induced changes in equilibrium distributions should not occur when these anions are present. Searle[38] has shown that water, chloride, nitrate, perchlorate, nor presumably hexafluorophosphate produce a separation of the three isomers of $[Co(dien)_2]^{3+}$ on SP-Sephadex chromatography columns. Therefore, isomer distributions determined with these species present should produce free energy differences approximating isolated-state values and in this context it is worth noting that distributions obtained with chloride, nitrate, and perchlorate present are all similar.[22]

(iv) Model for Electrochemical Reduction of Cobalt Complexes. Electrochemical data for kinetically inert systems such as $[Co(sep)]^{3+,2+}$ and $[Co(dien)_3]^{3+,2+}$ are amenable to a theoretical description. For many other complexes the cobalt(II) species is very labile and complicates the interpretation of data. Nevertheless, force field calculations on other systems demonstrate that minima in free energy do occur.[3,39-41] The electron-transfer scheme, under these conditions, must be interpreted in terms of reaction scheme 2. Support for this concept comes from data contained on other complexes in ref 42-44. Organic compounds studied by Evans et al. and other workers[45] also support this view.

The majority of studies describing the reduction process

$$Co(III) + e^- \overset{E^\circ, k_s, \alpha}{\rightleftharpoons} Co(II) \qquad (9)$$

treat the problem as a single step and no knowledge on conformer contribution is considered. This may be appropriate, fortuitously, as is the case of $[Co(sep)]^{3+,2+}$, where the same conformer is the most stable in both oxidation states, but if rearrangements of conformers with different E° values are involved in the electron transfer, then this cannot be correct. Studies are continuing in these laboratories to further understand the influence of conformation changes on redox processes. Clearly, homogeneous electron-transfer mechanisms are also affected by the above considerations, and importance of these concepts to this field will be considered at a later date.

Acknowledgment. Funding for the work described in this paper was provided by the Australian Research Grants Scheme and is gratefully acknowledged.

Registry No. $[Co(sep)]^{3+}$, 72496-77-6; $[Co(sep)]^{2+}$, 63218-22-4; *mer*-$[Co(dien)_2]^{3+}$, 38318-06-8; *mer*-$[Co(dien)_2]^{2+}$, 67145-46-4; *u-fac*-$[Co(dien)_2]^{3+}$, 38318-05-7; *u-fac*-$[Co(dien)_2]^{2+}$, 67145-47-5; *s-fac*-$[Co(dien)_2]^{3+}$, 38318-04-6; *s-fac*-$[Co(dien)_2]^{2+}$, 67145-48-6; $[Co(sep)](ClO_4)_3$, 88228-09-5.

(39) Hambley, T. W.; Hawkins, C. J.; Martin, J.; Palmer, J. A.; Snow, M. R. *Aust. J. Chem.* **1981**, *34*, 2505.
(40) Hambley, T. W.; Hawkins, C. J.; Palmer, J.; Snow, M. R. *Aust. J. Chem.* **1981**, *34*, 2525.
(41) Hambley, T. W.; Searle, G. H.; Snow, M. R. *Aust. J. Chem.* **1982**, *35*, 1285.
(42) Hanzlik, J.; Puxeddu, A.; Costa, G. *J. Chem. Soc., Dalton Trans.* **1977**, 542.
(43) Puxeddu, A.; Costa, G. *J. Chem. Soc., Dalton Trans.* **1977**, 2327.
(44) Ohsaka, T.; Oyama, N.; Yamaguchi, S.; Matsuda, H. *Bull. Chem. Soc. Jpn.* **1981**, *54*, 2475.
(45) Evans, D. H.; Busch, R. W. *J. Am. Chem. Soc.* **1982**, *104*, 5057 and references cited therein.

Contribution from Orion Research, Inc., Cambridge, Massachusetts 02139, and the Department of Biology, Syracuse University, Syracuse, New York 13210

Cadmium Binding by Biological Ligands. 3. Five- and Seven-Cadmium Binding in Metallothionein: A Detailed Thermodynamic Study

ALEX AVDEEF,*[1a] ANDRZEJ J. ZELAZOWSKI,[1b,c] and JUSTINE S. GARVEY*[1b]

Received July 6, 1984

The anaerobic binding of cadmium ions by rat liver apometallothionein 2 was studied by pH-static (pH 4.5, 6, 7, 8.25, 9.5), pCd-metric techniques, employing a microcomputer-controlled two-buret, two-electrode titrator. The solutions (3-4 mL, 25 °C, 0.15 M KNO_3) were 0.13-0.16 mM in apoprotein. Several of the sulfhydryl groups in metallothionein were found to be unexpectedly acidic, with pK_a's as low as 7. At pH 6 and 7 several cadmium-protein species were identified: the corresponding binding constants were successfully refined by a weighted nonlinear least-squares procedure. A dianionic seven-cadmium complex forms at pH 6, with an apparent binding constant of 10^{66}. Surprisingly, only five-cadmium complexes form if the apoprotein solution is reacted with cadmium ions at pH 7. At pH 6, 18 protons are liberated by the addition of metal ion, which is consistent with the displacement of all of the sulfhydryl protons by the metal ions. At pH 7, however, only 11 protons are liberated by the metal ions, clearly indicating that not all of the sulfhydryl groups participate in coordination, under the experimental conditions. A discussion of the possibility of a conformational change in the apoprotein taking place when the pH is raised from 6 to 7 is presented.

Introduction

Biologically significant sulfhydryl-containing ligands, such as cysteine, can strongly bind cadmium ions to form a variety of complexes whose compositions in aqueous solutions depend in a sensitive manner on such factors as pH, total cadmium ion concentration, ionic strength, and the presence of other metal ions and non-sulfhydryl ligands. Until recently, studies of cadmium reactions with sulfhydryl ligands had led to oversimplified models concerning the nature of complexes present in solution: the tendency of thiolate groups to bridge metal ions to form polynuclear complexes had been frequently neglected. Factors governing the stoichiometry and the extent of formation of polynuclear complexes in aqueous solution are consequently poorly understood. In parts 1 and 2 of this series, we applied novel potentiometric techniques to study the equilibrium mechanisms of cadmium binding with simple monosulfhydryl ligands: penicillamine[2] and cysteamine.[3] Both model systems were found to exhibit a tendency to form tri- and tetranuclear ternary complexes under mildly acidic conditions (pH 4-6). The present study concerns cadmium binding by the protein metallothionein (MT).

Metallothionein is a small (M_r 6700-6800) intracellular, sulfur-rich protein that strongly binds a variety of metal ions, including Zn, Cd, Cu, and Hg. The protein was first isolated from horse kidney by Margoshes and Vallee in 1957;[4] since then its

(1) (a) Orion Research. (b) Syracuse University. (c) Visiting Scientist, Institute of Environmental Research and Bioanalysis, Medical Academy of Lodz, Lodz, Poland.
(2) Avdeef, A.; Kearney, D. L. *J. Am. Chem. Soc.* **1982**, *104*, 7212-7218.
(3) Avdeef, A.; Brown, J. A. *Inorg. Chim. Acta* **1984**, *91*, 67-73.
(4) Margoshes, M.; Vallee, B. L. *J. Am. Chem. Soc.* **1957**, *79*, 4813-4814.

0020-1669/85/1324-1928$01.50/0